

We are IntechOpen, the world's leading publisher of Open Access books Built by scientists, for scientists

6,900

Open access books available

185,000

International authors and editors

200M

Downloads

Our authors are among the

154

Countries delivered to

TOP 1%

most cited scientists

12.2%

Contributors from top 500 universities



WEB OF SCIENCE™

Selection of our books indexed in the Book Citation Index
in Web of Science™ Core Collection (BKCI)

Interested in publishing with us?
Contact book.department@intechopen.com

Numbers displayed above are based on latest data collected.
For more information visit www.intechopen.com



Mechanism Design of Haptic Devices

Han Sung Kim¹
Kyungnam University¹
Republic of Korea¹

1. Introduction

The mechanism of a haptic device should have low inertia, high stiffness, large force reflection capability, good kinematic conditioning as well as large workspace, back-drivable, low friction, and small weight.

The first step of mechanism design is to select a proper mechanism structure (or type synthesis). For required DOF, several mechanism structures including serial-, parallel-, and hybrid-kinematic manipulators can be considered through type synthesis. Based on the previous review on haptic mechanisms (Martin and Savall, 2005), most successful haptic mechanisms are parallel-type and at least hybrid-type, due to low moving inertia, large force reflection and high stiffness. One of major disadvantages of parallel-kinematic manipulators may be smaller workspace compared to serial-kinematic counterparts. Joint and actuator types are also very important in type synthesis of haptic mechanisms. Most commercial haptic mechanisms use only revolute joints and rotary actuators, since those types can provide smaller friction, better back-drivability, and larger workspace than prismatic joints and linear actuators. In addition to linkage-type haptic devices, wire actuation (Agronin, 1987) and magnetic levitation (Berkelman et al., 1996) are also developed. In order to give broad information on mechanism structures to readers, novel mechanisms employed in haptic devices are classified by DOFs presented in Table 1 and the characteristics of each mechanism is briefly explained.

The second step of mechanism design is the dimensional synthesis of a selected mechanism structure. In the design of kinematic dimensions, workspace and other kinematic performances need to be considered together. The kinematic performance measures may be the manipulability, the inverse of condition number, the minimum force output, and so forth, which can be derived from the manipulator's Jacobian matrix. In general, workspace is inversely proportional to force transmission capability, accuracy and stiffness, which are closely related to the manipulability. Therefore, compromise between workspace volume and one of the kinematic performances related to manipulability should be included in the kinematic optimization.

This chapter is organized as follows. In section 2, novel mechanism structures employed in haptic devices are explained. In section 3, the methodologies of kinematic analysis and optimization are presented. In section 4, example of kinematic analysis and design of the Delta haptic device is illustrated.

2. Mechanism Structures

In this section, a state of the art in mechanisms of haptic devices is presented from planar to spatial mechanisms. Once required degrees of freedom (DOF) of a haptic device is specified, several feasible mechanisms to satisfy specified DOF can be synthesized (Tsai, 2001; Kong & Gosselin, 2007; Gogu, 2008). The degrees of freedom, F , of a mechanism can be easily calculated by well-known Grubler’s formula as (Tsai, 1999)

$$F = \lambda(n - j - 1) + \sum_{i=1}^j f_i$$

(1)

where

- λ : degrees of freedom of the space
- n : number of links including the fixed link
- j : number of joints
- f_i : degrees of relative motion by joint i .

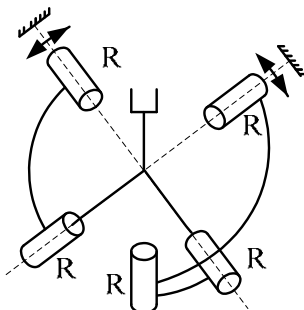
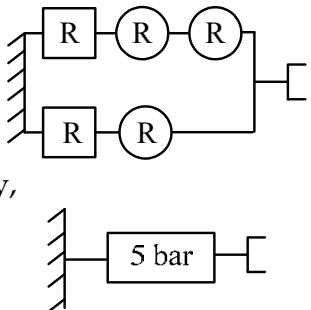
However, degrees of freedom can be simply calculated for serial- and parallel-kinematic manipulators as follows:

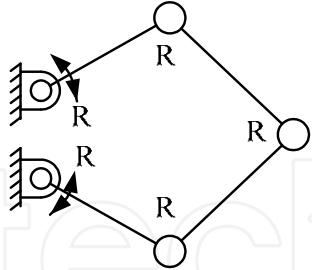
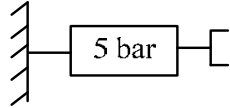
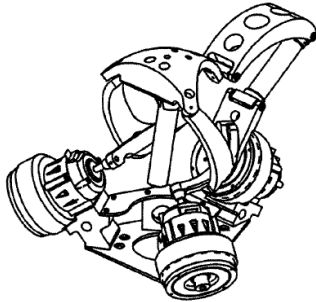
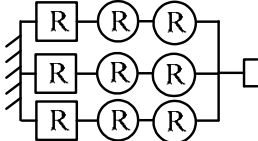
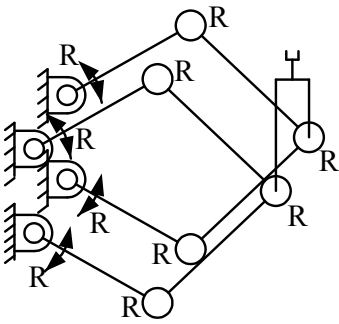
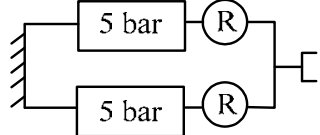
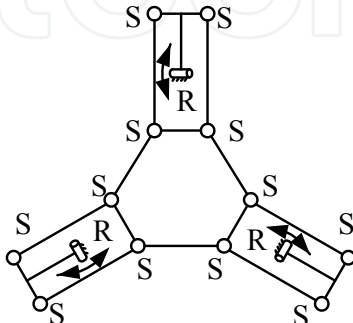
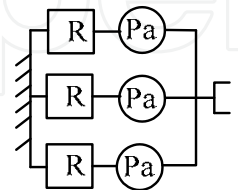
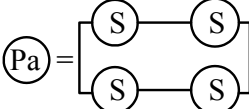
$$F = \sum_{i=1}^j f_i \quad \text{for serial manipulators}$$

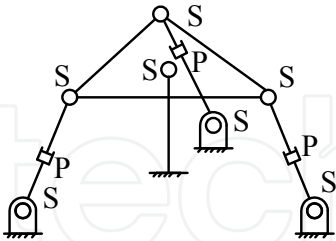
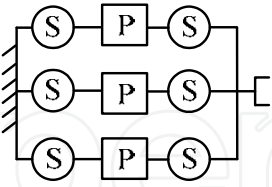
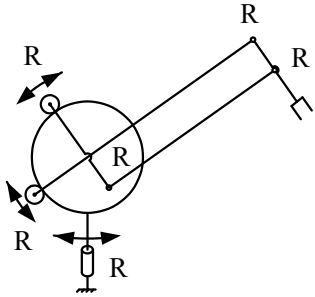
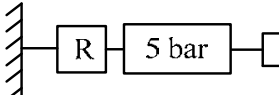
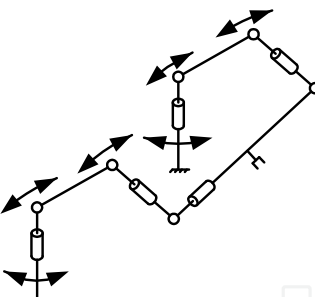
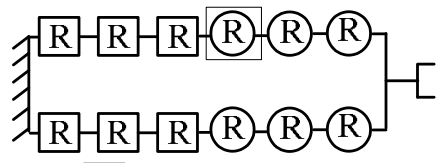

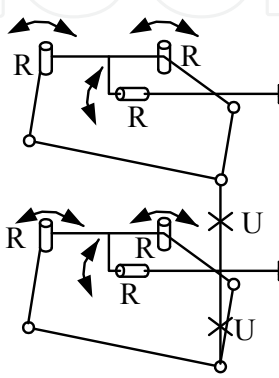
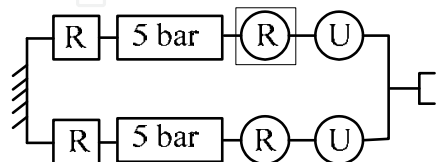

$$F = \lambda - \sum_{i=1}^m c_i \quad \text{for parallel manipulators}$$

(2)

where c_i denotes the total number of independent constraints of the i th leg consisting of a parallel manipulators with m legs. Note that for serial manipulators, the first term in Eq. (1) always becomes zero. For example, 5-bar can be considered as a planar parallel manipulator with two legs, then $F = \lambda - (c_1 + c_2) = 2$ where $\lambda = 3$, $c_1 = \lambda - 3 = 0$, and $c_2 = \lambda - 2 = 1$. Another example is a spatial parallelogram with two S-S (spherical-spherical) chains. The parallelogram has $F = \lambda - (c_1 + c_2) = 4$, since $\lambda = 6$ and $c_i = \lambda - 5 = 1$ for $i = 1, 2$. Note that one rotational DOF along the leg is passive DOF (Tsai, 1999). Table 1 shows mechanism structures of developed haptic devices and mechanism structures are classified by DOFs.

2- DOF	[Spherical 5-bar] - Spherical Remote-Center-of-Motion Manipulator for MIS (Angerilli et al., 2001) - Immersion Impulse Engine 2000 (Rosenberg & Jackson, 2002)	
		<div>Shortly,</div> 

2- DOF	[Planar 5-bar] - The Pantograph (Campion et al., 2005)	
		
3- DOF	[Spherical mechanism] - SHaDe (Birglen et al., 2002)	
		
3- DOF	[Two Planar 5-bars] - 3-DOF Planar Pantograph Interface (Sirouspour et al., 2000)	
		
3- DOF	[Spatial Parallelograms] - Delta Haptic Device (Grange et al., 2001, http://www.forcedimension.com)	
		 <p>where,</p> 

3-DOF	[Wrist Mechanism for the Delta Haptic device] - Connecting the wrist on the Delta haptic device for 6-DOF motion. - Instead of the linkages of S-P-S chains, wires are used.	
		
3-DOF	[Hybrid Manipulator] - PHANTOM Desktop/Omni (Cavusolgu et al., 2002; http://www.sensable.com)	
		
5,6-DOF	[Two PHANTOMS Configuration] - Connecting two PHANTOM devices by a 5- or 6-DOF serial Chain (Wang, 2001; Iwata, 1993)	
		 where,  may be actuated for 6-DOF
5,6-DOF	[Twin Pantographs] - 5-DOF Haptic Wand (Stocco, 2001, http://www.quanser.com)	
		 where,  may be actuated for 6-DOF

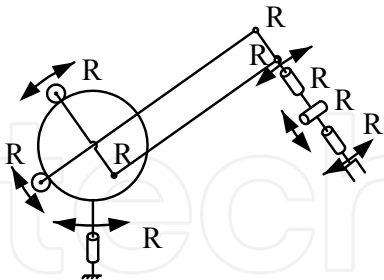
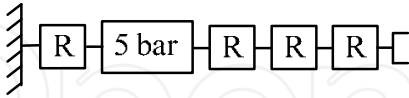
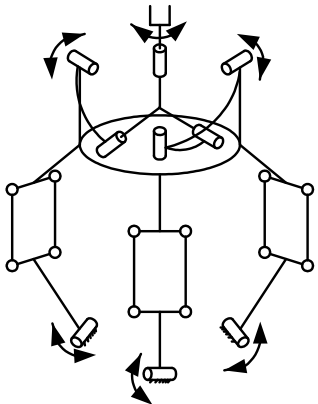
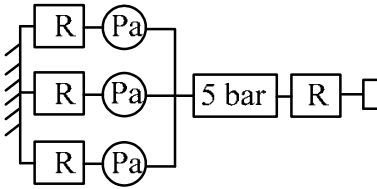
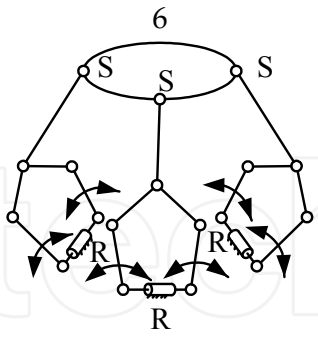
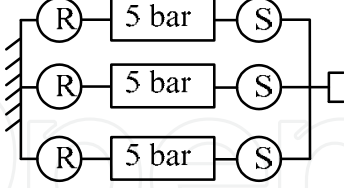
6-DOF	[Serial Manipulator] - PHANTOM Premium 1.5/6DOF (Chen, 1999; Cohen & Chen, 1999) - Actually, it is a hybrid-kinematic manipulator.	
		
6-DOF	[Hybrid Manipulator] - Compact 6-DOF Haptic Interface (Tsumaki et al., 1998; Yoon, 2003)	
		
6-DOF	[Three Pantographs] (Long & Collins, 1992)	
		
6~10 DOF	[Serial Manipulators] - ViSHaRD6 (Ueberle & Buss, 2002) - ViSHaRD10 (Ueberle et al, 2004) - Freedom6s (http://www.mpb-technologies.ca) - Freedom-7 (Hayward, 1995; Hayward et al., 1997)	

Table 1. Mechanism structures of currently developed haptic devices

3. Kinematic analysis and optimization

The overall process of haptic rendering is shown in Figure 1. First, according to operator's movement, the controller of a haptic device system measures joint displacements and calculates the tip (or end-effector of a haptic device) position and velocity by forward kinematics and velocity relation, respectively. Then, the position and velocity commands are sent to virtual environments or real tele-operated robots and the contact force between tool and environment is calculated or measured. Finally, the required actuation force to realize the contact force is calculated through the statics relation of a haptic device. Note that scaling or mapping between the measured and commanded positions/forces may be required.

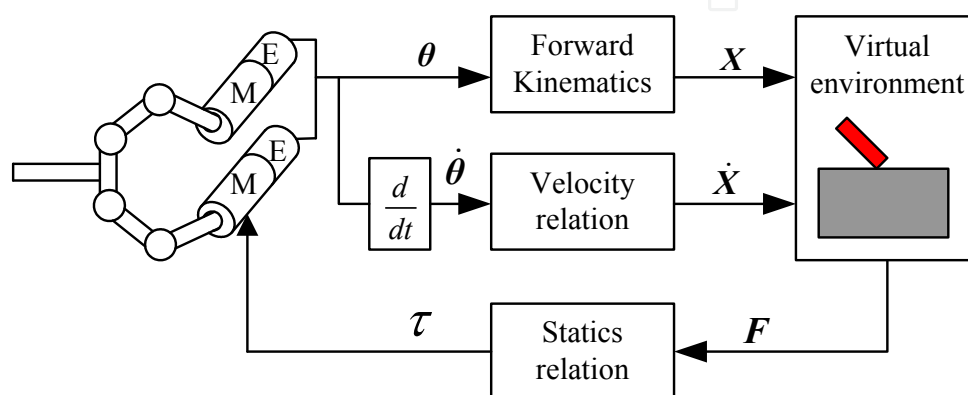


Fig. 1. Schematic diagram of haptic rendering cycle

3.1 Kinematic analysis

In this subsection, brief explanation of the kinematic analysis will be given. For the haptic rendering cycle, the analyses of forward/inverse kinematics and velocity/statics relations are required. The analysis of inverse kinematics is not directly used in the cycle; however it is required in the calculation of the Jacobian matrix especially for parallel manipulators.

In general, the forward kinematics of an n -DOF serial manipulator can be calculated by multiplying the Denavit-Hartenberg homogeneous transformation matrices, ${}^{i-1}T_i(\theta_i)$, from the base coordinate system to the end-effector coordinate system in series.

$${}^0T_n = {}^0T_1(\theta_1) {}^1T_2(\theta_2) \cdots {}^{n-1}T_n(\theta_n) \quad (3)$$

The velocity and statics relations of an n -DOF serial manipulator are given by

$$\dot{X} = J\dot{\theta} \quad \text{and} \quad \tau = J^T F \quad (4)$$

where $\dot{X} = [\mathbf{v}^T, \boldsymbol{\omega}^T]^T$ when \mathbf{v} and $\boldsymbol{\omega}$ denote the linear and angular velocity vectors and $F = [\mathbf{f}^T, \mathbf{m}^T]^T$ when \mathbf{f} and \mathbf{m} are the force and moment vectors. The column vectors of Jacobian matrix consist of the joint screws expressed in the axis coordinates (Duffy, 1996).

$$J = \begin{bmatrix} \mathbf{r}_1 \times \mathbf{s}_1 & \cdots & \mathbf{r}_n \times \mathbf{s}_n \\ \mathbf{s}_1 & \cdots & \mathbf{s}_n \end{bmatrix} \quad (5)$$

where \mathbf{s}_i denotes the unit direction vector of the i th joint axis and \mathbf{r}_i is the position vector from the end-effector to the i th joint axis.

On the other hands, the forward kinematics of an n -DOF parallel manipulator is not straightforward and has multiple solutions in general. However, the inverse kinematics is much simpler and can be analyzed by using vector-loop equations. The velocity and statics relations of an n -DOF parallel manipulator are given by

$$\dot{\boldsymbol{\theta}} = J^T \dot{\mathbf{X}} \text{ and } \mathbf{F} = J \boldsymbol{\tau} \quad (6)$$

where $J = J_x J_\theta^{-1}$. Here, J_θ is the diagonal matrix and becomes an $n \times n$ identity matrix if actuators are linear. The column vectors of J_x consist of the joint screws expressed in the ray coordinates (Duffy, 1996).

$$J_x = \begin{bmatrix} \mathbf{s}_1 & \cdots & \mathbf{s}_n \\ \mathbf{r}_1 \times \mathbf{s}_1 & \cdots & \mathbf{r}_n \times \mathbf{s}_n \end{bmatrix} \quad (7)$$

3.2 Kinematic optimization

In the preliminary design of a haptic device, large workspace volume, high force transmission capability, high accuracy and high stiffness are essential considerations. In general, the workspace is inversely proportional to force transmission capability, accuracy and stiffness, which are closely related to the manipulability. Therefore, compromise between workspace volume and one of the performances related to manipulability are required in the kinematic optimization.

First, the closed form solution for workspace cannot be obtained for most spatial manipulators. Usually, workspace is calculated numerically by using the inverse kinematics considering actuator strokes and joint limits.

Some kinematic performance measures such as manipulability, force/velocity transmission capability, accuracy and stiffness can be derived from the manipulator's Jacobian matrix. Some of well-known kinematic performance measures are

- manipulability: the product of the singular values of the Jacobian matrix (Yoshikawa, 1985)
- mechanism isotropy: the inverse of the condition number of the Jacobian matrix or the ratio of the smallest to the largest singular value of the Jacobian matrix (Salisbury & Craig, 1982)
- minimum force (or velocity) output: the smallest singular value or the force (or velocity) output in the worst direction (Kim & Choi, 2001).

One of the measures can be used as LDI (Local Design Index), which means the kinematic performance at one configuration in workspace. The average value of LDI over whole workspace can be obtained by (Gosselin and Angeles, 1989; Kim and Tsai, 2003)

$$\text{GDI}(\boldsymbol{\beta}) = \frac{1}{W} \int_W \text{LDI}(\boldsymbol{\beta}) dW \quad (8)$$

where W and dW denote the total workspace volume and a differential workspace, respectively, and $\boldsymbol{\beta}$ denotes design variables or kinematic dimensions. The sum of LDI over workspace can be normalized by the workspace size, which yields a kinematic performance measure independent of different workspace volume of design candidates. Therefore, it is usually called GDI (Global Design Index). However, maximizing the GDI alone usually leads to very small workspace, while maximizing workspace generates poor kinematic performances. Hence, the optimal design problem may be formulated as

$$\begin{aligned} &\text{Maximize : } \text{GDI}(\boldsymbol{\beta}) \\ &\text{Subject to : } W \geq W_{\min} \end{aligned} \quad (9)$$

where W_{\min} denotes the minimum required workspace volume. The physical meaning is to maximize the average value of a selected kinematic performance measure over whole workspace while guaranteeing the minimum required workspace volume.

4. Example of the kinematic optimization of a Delta haptic device

In this section, the kinematic analysis and optimization methods for a haptic device are illustrated with the Delta haptic device. As explained in section 2, the Delta mechanism consists of three *R-Pa* (Revolute-spatial Parallelogram) legs. Since each leg has one rotational constraint (or rotation about the normal vector of the plane made by each parallelogram), the combined effects result in three constraints of the rotation of the moving platform. Therefore, the moving platform has three translational degrees of freedom.

As shown in Figure 2, fixed reference frame (x, y, z) is attached to the center O of the fixed base. Local fixed frame (x_i, y_i, z_i) is attached to the fixed base at point A_i . The moving frame (u, v, w) is also attached the center P of the moving platform. The angle, ϕ_i , is defined as the angle from the x -axis to the x_i -axis. In Figure 3, the joint angles, $\theta_{1i}, \theta_{2i}, \theta_{3i}$ for the i th leg are defined. A vector-loop equation can be written for each leg:

$$\overline{A_i M_i} + \overline{M_i B_i} = \overline{OP} + \overline{PB_i} - \overline{OA_i} \quad \text{or} \quad l_{1i} \mathbf{u}_{1i} + l_{2i} \mathbf{u}_{2i} = \mathbf{p} + \mathbf{b} - \mathbf{a} . \quad (10)$$

The vector-loop equation can be expressed in local frame (x_i, y_i, z_i) as

$$\begin{bmatrix} l_{1i}c\theta_{1i} + l_{2i}s\theta_{3i}c(\theta_{1i} + \theta_{2i}) \\ l_{2i}c\theta_{3i} \\ l_{1i}s\theta_{1i} + l_{2i}s\theta_{3i}s(\theta_{1i} + \theta_{2i}) \end{bmatrix} = \begin{bmatrix} b_{xi} \\ b_{yi} \\ b_{zi} \end{bmatrix} \tag{11}$$

where

$$\begin{bmatrix} b_{xi} \\ b_{yi} \\ b_{zi} \end{bmatrix} = \begin{bmatrix} c\phi_i & s\phi_i & 0 \\ -s\phi_i & c\phi_i & 0 \\ 0 & 0 & 1 \end{bmatrix} \begin{bmatrix} p_x \\ p_y \\ p_z \end{bmatrix} + \begin{bmatrix} b-a \\ 0 \\ 0 \end{bmatrix} \tag{12}$$

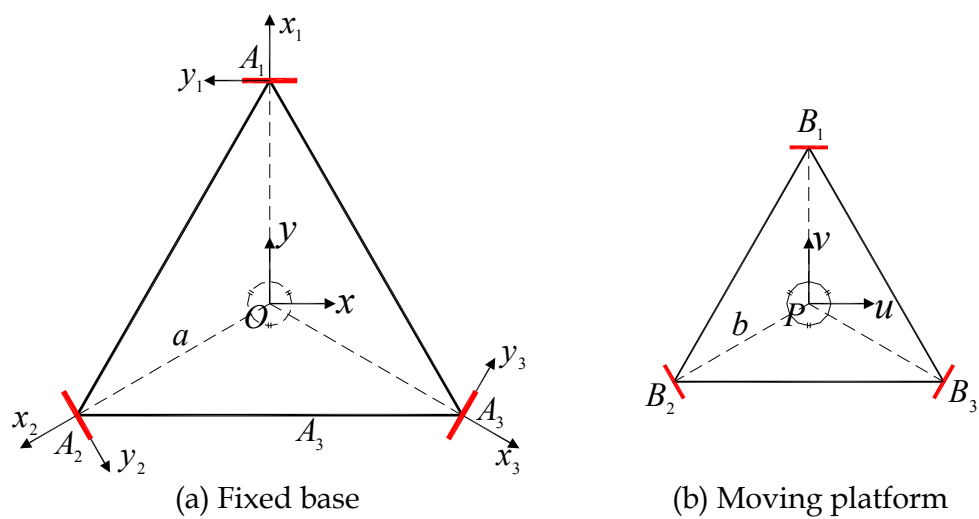


Fig. 2. Top views of the Delta manipulator

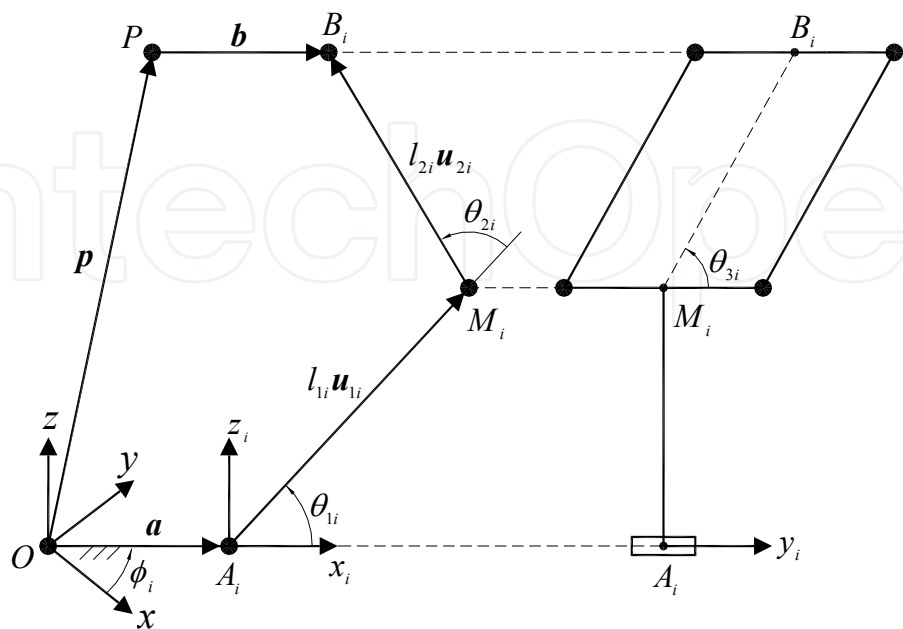


Fig. 3. Vector-loop diagram of the *i*th leg

The problem of inverse kinematics is to find the actuated joint angle, $\theta_{1i}, \theta_{2i}, \theta_{3i}$ for given the position vector, \mathbf{p} , of the moving platform. From the second element of Eq. (11), θ_{3i} is obtained by

$$\theta_{3i} = \cos^{-1} \frac{b_{yi}}{l_{2i}}. \quad (13)$$

Summing the squares of b_{xi} , b_{yi} , and b_{zi} in Eq. (11) and solving for θ_{2i} yields

$$\theta_{2i} = \cos^{-1} \kappa \quad (14)$$

where $\kappa = (b_{xi}^2 + b_{yi}^2 + b_{zi}^2 - l_{1i}^2 - l_{2i}^2) / (2l_{1i}l_{2i}s\theta_{3i})$. Note that θ_{3i} and θ_{2i} has two solutions, respectively, however only positive values are selected. Once θ_{3i} and θ_{2i} are determined, θ_{1i} can be obtained from Eq. (11) by

$$\theta_{1i} = \text{Atan2}(-g_{2i}b_{xi} + g_{1i}b_{zi}, g_{1i}b_{xi} + g_{2i}b_{zi}) \quad (15)$$

where $g_{1i} \equiv l_{1i} + l_{2i}c\theta_{2i}s\theta_{3i}$ and $g_{2i} \equiv l_{2i}s\theta_{2i}s\theta_{3i}$.

The forward kinematics problem is to find the position vector, \mathbf{p} , of the moving platform for given the actuated joint angle, $\theta_{1i}, \theta_{2i}, \theta_{3i}$. Geometrically, the point, P , is calculated as the intersection point of three spheres centered at M'_i , which is located at a distance b from M_i in the direction of $\overline{B_iP}$. The detailed derivation can be referred to that of the Maryland Manipulator (Tsai, 1999).

The Jacobian matrix can be derived by differentiating Eq. (10) as

$$\mathbf{v}_p = l_{1i}(\boldsymbol{\omega}_{1i} \times \mathbf{u}_{1i}) + l_{2i}(\boldsymbol{\omega}_{2i} \times \mathbf{u}_{2i}) \quad (16)$$

where \mathbf{v}_p is the linear velocity of the moving platform and $\boldsymbol{\omega}_{ji}$ is the angular velocity of the j th link of the i th leg. To eliminate the passive joint rate, dot-multiplying both sides of Eq. (16) by \mathbf{u}_{2i} yields

$$\mathbf{u}_{2i} \cdot \mathbf{v}_p = l_{1i}\boldsymbol{\omega}_{1i} \cdot (\mathbf{u}_{1i} \times \mathbf{u}_{2i}) \quad (17)$$

Expressing the vectors in Eq. (17) in the local frame (x_i, y_i, z_i) gives

$${}^i\boldsymbol{\omega}_{li} = \begin{bmatrix} 0 \\ -\dot{\theta}_{li} \\ 0 \end{bmatrix}, {}^i\boldsymbol{u}_{li} = \begin{bmatrix} c\theta_{li} \\ 0 \\ s\theta_{li} \end{bmatrix}, {}^i\boldsymbol{u}_{2i} = \begin{bmatrix} s\theta_{3i}c(\theta_{li} + \theta_{2i}) \\ c\theta_{3i} \\ s\theta_{3i}s(\theta_{li} + \theta_{2i}) \end{bmatrix}, {}^i\boldsymbol{v}_p = \begin{bmatrix} v_{px}c\phi_i + v_{py}s\phi_i \\ -v_{px}s\phi_i + v_{py}c\phi_i \\ v_{pz} \end{bmatrix} \quad (18)$$

Substituting Eq. (18) into Eq. (17) and applying the result for $i=1, 2$, and 3 , the velocity relation can be derived by

$$\boldsymbol{J}_x^T \boldsymbol{v}_p = \boldsymbol{J}_q \dot{\boldsymbol{\theta}} \quad \text{or} \quad \dot{\boldsymbol{\theta}} = \boldsymbol{J}^T \boldsymbol{v}_p \quad (19)$$

where $\boldsymbol{J} = \boldsymbol{J}_x \boldsymbol{J}_\theta^{-1}$,

$$\boldsymbol{J}_x = \begin{bmatrix} j_{1x} & j_{2x} & j_{3x} \\ j_{1y} & j_{2y} & j_{3y} \\ j_{1z} & j_{2z} & j_{3z} \end{bmatrix}, \text{ and } \boldsymbol{J}_q = \begin{bmatrix} l_{11}s\theta_{21}s\theta_{31} & 0 & 0 \\ 0 & l_{12}s\theta_{22}s\theta_{32} & 0 \\ 0 & 0 & l_{13}s\theta_{23}s\theta_{33} \end{bmatrix} \quad (20)$$

where

$$\begin{aligned} j_{ix} &= c(\theta_{li} + \theta_{2i})s\theta_{3i}c\phi_i - c\theta_{3i}s\phi_i \\ j_{iy} &= c(\theta_{li} + \theta_{2i})s\theta_{3i}s\phi_i + c\theta_{3i}c\phi_i \\ j_{iz} &= s(\theta_{li} + \theta_{2i})s\theta_{3i} \end{aligned} \quad (21)$$

The design variables of the Delta manipulator can be radii of the fixed base and the moving platform, (a, b) , and lengths of lower and upper legs, (l_1, l_2) . For symmetrical design, all the legs are set to be identical, i.e., $l_j = l_{ji}$ for $i=1, 2, 3$. Therefore, the design variables become

$$\boldsymbol{\beta} = [a, b, l_1, l_2] \quad (22)$$

Furthermore, the design variables may be normalized by a characteristic length, a , as

$$\tilde{\boldsymbol{\beta}} = \left[\frac{b}{a}, \frac{l_1}{a}, \frac{l_2}{a} \right] \quad (23)$$

In this optimal design problem, the minimum force output is selected as a LDI. The physical meaning of the index corresponds to the maximum magnitude of the force vector which can be generated in all directions at the end-effector for given unit magnitude of actuator forces (Kim and Choi, 2001). The problem of determining the extreme magnitudes of the force vector at the end-effector when the magnitude of actuator forces is constrained can be formulated as follow:

$$\begin{aligned} \text{Maximize: } & \|F\|^2 = F^T F \\ \text{Subject to: } & \|\tau\|^2 = F^T (JJ^T)^{-1} F = 1 \end{aligned} \quad (24)$$

Applying the Lagrange multipliers yields the following eigenvalue problem:

$$(JJ^T)F = \alpha_f^2 F \quad (25)$$

The minimum force output for given unit magnitude of actuator forces can be obtained as the square root of the minimum eigenvalue of JJ^T . Hence, the optimal design problem is formulated as

$$\begin{aligned} \text{Maximize: } & \text{GDI}(\tilde{\beta}) = \frac{1}{W} \int_W \text{LDI}(\tilde{\beta}) dW \\ \text{Subject to } & : W \geq W_{\min} \end{aligned} \quad (26)$$

In this numerical example, the ranges of the normalized design variables and the minimum workspace volume are set to

$$0.1 \leq \frac{b}{a} \leq 1.0, \quad 0.5 \leq \frac{l_1}{a} \leq 2.5, \quad 0.5 \leq \frac{l_2}{a} \leq 2.5, \quad \text{and } W_{\min} = 0.008 m^3$$

where $a = 100 \text{ mm}$.

Figure 4 shows the workspace volume and LDI with respect to l_1 and l_2 when $b = 20 \text{ mm}$. As expected, the workspace volume is increasing as l_1 and l_2 are larger, however the LDI is larger when l_1 is smaller, because actuated force at M_i is larger when l_1 is smaller. Genetic algorithm in Matlab is used to search optimal design variables based on Eq. (26). The result is obtained by

$$b = 17.3, l_1 = 73.2, l_2 = 209.5 \text{ mm}.$$

Figure 5 shows the mechanism at $(0, 0, 200) \text{ mm}$ and the workspace volume of the optimized Delta haptic device.

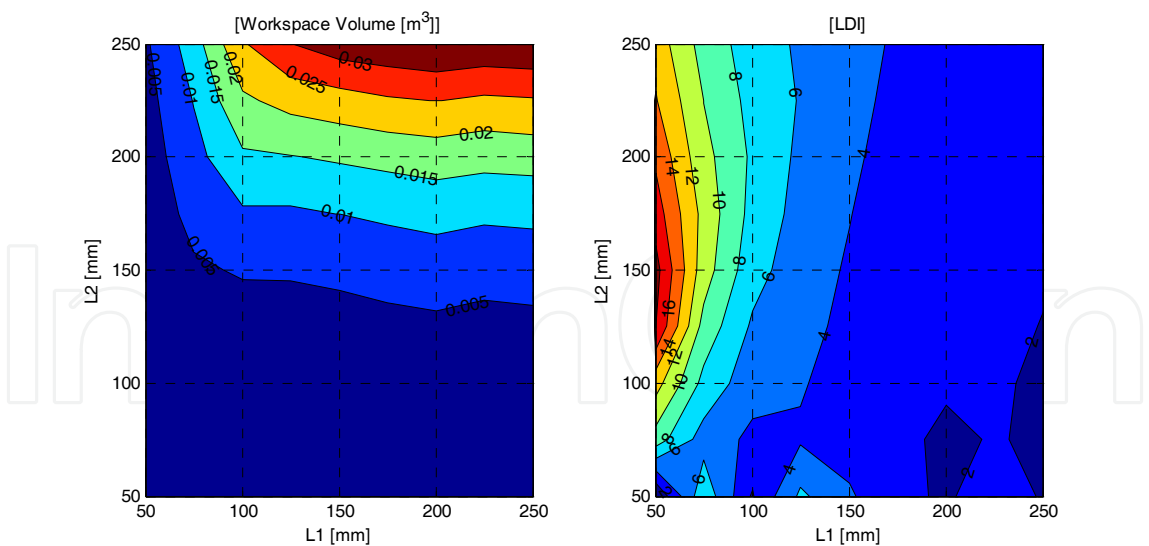


Fig. 4. Contour plots of workspace and LDI with respect to l_1 and l_2 for $b = 20\text{ mm}$

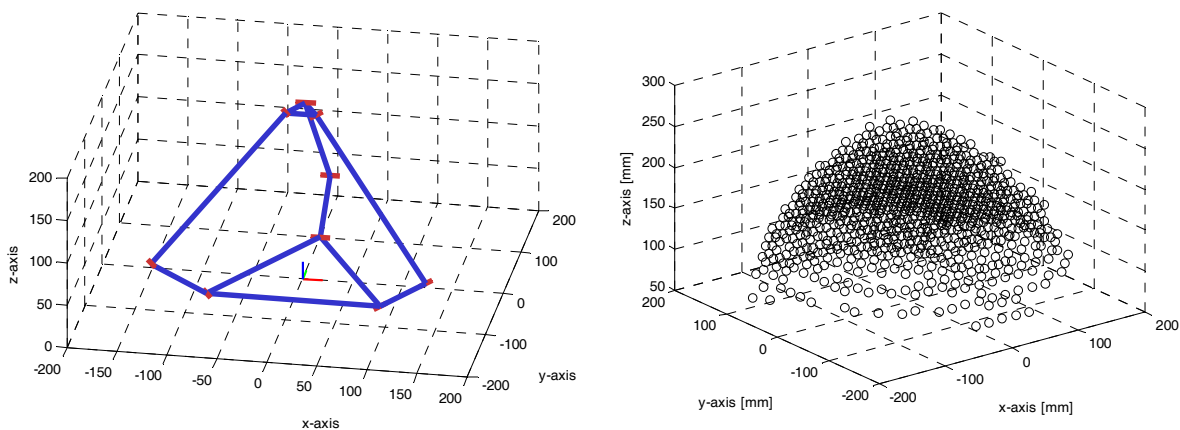


Fig. 5. Configuration at $(0, 0, 200)\text{ mm}$ and workspace volume of the optimized Delta haptic device

5. Conclusions

This chapter discuss recent development of novel mechanism structures used in haptic device. The kinematic analysis methods of serial- and parallel-kinematic manipulators for haptic rendering cycle are presented and some important kinematic measures are suggested. The procedure of kinematic optimization of haptic mechanisms is presented. Example of the Delta haptic device shows the effectiveness of the kinematic optimization.

6. References

Martin, J. & Savall, J. (2005), Mechanism for Haptic Torque Feedback, *Proceedings of the First Joint Eurohaptics Conference and Symposium on Haptic Interfaces for Virtual Environment and Teleoperator System*.

- Agronin, M. L. (1987), The Design of a Nine-string Six-degree-of-freedom Force-feedback Joystick for Telem Manipulation, *Proceedings of the NASA Workshop on Space Telerobotics*, pp. 341-348.
- Berkelman, P. J.; Butler, Z. & Hollis, R. L. (1996), Design of a Hemispherical Magnetic Levitation Haptic Interface, *Proceedings of the ASME Dynamics Systems and Control Division*, Vol. 58, pp. 483-488.
- Tsai, L. W. (1999), *Robot Analysis: The Mechanics of Serial and Parallel Manipulators*, John Wiley & Sons, Canada.
- Tsai, L. W. (2001). *Mechanism Design: Enumeration of Kinematic Structures According to Function*, CRC press.
- Kong, X. & Gosselin, C. (2007). *Type Synthesis of Parallel Mechanisms*, Springer, Netherlands.
- Gogu, G. (2008). *Structural Synthesis of Parallel Robots*, Springer, Netherlands.
- Angerilli, M.; Frisoli A. & Salsedo, F. & Marcheschi, S. & Bergamasco, M. (2001), Haptic Simulation of an Automotive Manual Gearshift, *Proceedings of the IEEE International Workshop on Robot and Human Interactive Communication*.
- Rosenberg, L. B. & Jackson, B. G. (2002), Force Feedback Device Including Flexure Member Between Actuator and User Object, *United States Patent 6437771*.
- Campion, G.; Wang, Q. & Hayward, V. (2005), The Pantograph Mk-II: A Haptic Instrument, *Proc. IROS 2005, IEEE/RSJ Int. Conf. Intelligent Robots and Systems*, pp. 723-728.
- Birglen, L.; Gosselin, C. & Pouliot, N. & Monsarrat, B. & Laliberte, T. (2002), SHaDe, A New 3-DoF Haptic Device, *IEEE Transactions on Robotics and Automation*, Vol. 18, pp. 166-175.
- Sirouspour, M. R.; DiMaio, S. P. & Salcudean, S. E. & Abolmaesumi, P. & Jones, C. (2000), Haptic Interface Control - Design Issues and Experiments with a Planar Device, *Proceedings of the IEEE International Conference on Robotics & Automation*.
- Grange S.; Conti F. & Helmer P. & Rouiller P. & Baur C. (2001), The Delta Haptic Device as a Nanomanipulator, *SPIE Microrobotics and Microassembly III*, Boston, MA.
- Cavusoglu, M. C.; Feygin D. & Tendick, F. (2002), A Critical Study of the Mechanical and Electrical Properties of the PHANTOM Haptic Interface and Improvements for High-Performance Control, *The MIT Press Journals*, Vol. 11, No. 6, pp. 555-568.
- Wang S. (2001), *Role of torque in haptic perception of virtual objects*, Thesis S M, Dept of Mechanical Engineering, Massachusetts Institute of Technology.
- Iwata H. (1993), Pen-Based Haptic Virtual Environment, *Proceedings of the IEEE Virtual Reality Annual International Symposium*, Seattle, Washington, pp. 287- 292.
- Stocco, L. J.; Salcudean, S. E. & Sassani, F. (2001), Optimal Kinematic Design of a Haptic Pen, *IEEE/ ASME Transactions on Mechatronics*, Vol. 6, No. 3, pp. 210-220.
- Chen, E. (1999), Six Degree-of-Freedom Haptic System For Desktop Virtual Prototyping Applications, *Proceedings of the International Workshop on Virtual Reality and Prototyping*, Laval, France, pp. 97-106.
- Cohen A. & Chen, E. (1999), Six Degree-of-Freedom Haptic System as a Desktop Virtual Prototyping Interface, *Proceedings of the ASME Winter Annual Meeting, Dynamics Systems and Control*, Nashville, Tennessee, Vol. 67, pp. 401-402.
- Tsumaki, Y.; Naruse, H. & Nenchev, D. N. & Uchiyama, M. (1998), Design of a Compact 6-DoF Haptic Interface, *Proceedings of the IEEE International Conference on Robotics & Automation*, pp. 2580-2585.

- Yoon, W. K.; Suehiro, T. & Tsumaki, Y. & Uchiyama, M. (2003), A Compact Modified Delta Parallel Mechanism Design based on Stiffness Analysis, *Proceedings of the 2003 IEEE/ASME International Conference on Advanced Intelligent Mechatronics*, pp. 1262-1267.
- Long, G. L. & Collins, C. L. (1992), A Pantograph Linkage Parallel Platform Master Hand Controller for Force- Reflection, *Proceedings of the IEEE International Conference on Robotics and Automation*, Nice, France, pp. 390-395.
- Hayward, V. (1995), Toward a Seven Axis Haptic Interface, *Proceedings of the IROS International Workshop on Intelligent Robots and Systems*, Vol. 2, pp. 133-139.
- Hayward, V.; Gregorio, P. & Astley, O. R. & Greenish, S. & Doyon, M. (1997), Freedom-7: A High Fidelity Seven Axis Haptic Device With Application To Surgical Training, *Proceedings of the ISER 6th International Symposium on Experimental Robotics*, Vol. 5.
- Ueberle, M. & Buss, M. (2002), Design, Control, and Evaluation of a New 6 DOF Haptic Device, *Proceedings of the IEEE International Conference on Intelligent Robots and Systems*, Lausanne, Switzerland, pp. 2949-2954.
- Ueberle, M.; Mock, N. & Buss, M. (2004), ViSHaRD10, a Novel Hyper-Redundant Haptic Interface, *Proceedings of the IEEE 12th International Symposium on Haptic Interfaces for Virtual Environment and Teleoperator Systems*, Chicago, Illinois, USA, pp. 58- 65.
- Duffy, J. (1996), *Statics and Kinematics with applications to Robotics*, Cambridge University Press, pp. 89-156.
- Yoshikawa, T. (1985), Manipulability of Robotic Mechanisms, *International Journal of Robotics Research*, Vol. 4, No. 2, pp. 3-9.
- Salisbury, J. K. & Craig, J. J. (1982), Articulated Hands: Force Control and Kinematics Issues, *International Journal of Robotics Research*, Vol. 1, No. 1, pp. 4-17.
- Kim, H. S. & Choi, Y. J. (2001), Forward/Inverse Force Transmission Capability Analyses of Fully Parallel Manipulators, *IEEE Transaction on Robotics and Automation*, Vol. 17, No. 4, pp. 526-530.
- Kim, H. S. & Tsai, L. W. (2003), Design Optimization of a Cartesian Parallel Manipulator, *Journal of Mechanical Design*, Vol. 125, No. 1, pp.43-51.
- Gosselin, C. & Angeles, J. (1989), The Optimum Kinematic Design of a Spherical Three-Degrees-of-Freedom Parallel Manipulator, *ASME Journal of Mechanisms, Transmissions and Automation in Design*, Vol. 111, No. 2, pp. 202-207.

IntechOpen

IntechOpen



Advances in Haptics

Edited by Mehrdad Hosseini Zadeh

ISBN 978-953-307-093-3

Hard cover, 722 pages

Publisher InTech

Published online 01, April, 2010

Published in print edition April, 2010

Haptic interfaces are divided into two main categories: force feedback and tactile. Force feedback interfaces are used to explore and modify remote/virtual objects in three physical dimensions in applications including computer-aided design, computer-assisted surgery, and computer-aided assembly. Tactile interfaces deal with surface properties such as roughness, smoothness, and temperature. Haptic research is intrinsically multi-disciplinary, incorporating computer science/engineering, control, robotics, psychophysics, and human motor control. By extending the scope of research in haptics, advances can be achieved in existing applications such as computer-aided design (CAD), tele-surgery, rehabilitation, scientific visualization, robot-assisted surgery, authentication, and graphical user interfaces (GUI), to name a few. *Advances in Haptics* presents a number of recent contributions to the field of haptics. Authors from around the world present the results of their research on various issues in the field of haptics.

How to reference

In order to correctly reference this scholarly work, feel free to copy and paste the following:

Han Sung Kim (2010). Mechanism Design of Haptic Devices, *Advances in Haptics*, Mehrdad Hosseini Zadeh (Ed.), ISBN: 978-953-307-093-3, InTech, Available from: <http://www.intechopen.com/books/advances-in-haptics/mechanism-design-of-haptic-devices>

INTECH
open science | open minds

InTech Europe

University Campus STeP Ri
Slavka Krautzeka 83/A
51000 Rijeka, Croatia
Phone: +385 (51) 770 447
Fax: +385 (51) 686 166
www.intechopen.com

InTech China

Unit 405, Office Block, Hotel Equatorial Shanghai
No.65, Yan An Road (West), Shanghai, 200040, China
中国上海市延安西路65号上海国际贵都大饭店办公楼405单元
Phone: +86-21-62489820
Fax: +86-21-62489821

© 2010 The Author(s). Licensee IntechOpen. This chapter is distributed under the terms of the [Creative Commons Attribution-NonCommercial-ShareAlike-3.0 License](https://creativecommons.org/licenses/by-nc-sa/3.0/), which permits use, distribution and reproduction for non-commercial purposes, provided the original is properly cited and derivative works building on this content are distributed under the same license.

IntechOpen

IntechOpen